Pyrolysis of Epoxy Resins and Fire Behavior of Epoxy Resin Composites Flame-Retarded with 9,10-Dihydro-9-oxa-10-phosphaphenanthrene-10-oxide Additives

B. Schartel,[1] A. I. Balabanovich,[1] U. Braun,[1] U. Knoll,[1] J. Artner,[2] M. Ciesielski,[2] M. Döring,[2] R. Perez,[3] J. K. W. Sandler,[3] V. Altstädt,[3] T. Hoffmann,[4] D. Pospiech[4]

[1]*Federal Institute for Materials Research and Testing, Unter den Eichen 87, 12205 Berlin, Germany*
[2]*Institute of Technical Chemistry, Research Center Karlsruhe GmbH, 76021 Karlsruhe, Germany*
[3]*Department of Polymer Engineering, University of Bayreuth, Universitätsstraβe 30, 95447 Bayreuth, Germany*
[4]*Leibniz-Institute of Polymer Research Dresden, Hohe Str. 6, 01069 Dresden, Germany*

Received 11 August 2006; accepted 12 October 2006
DOI 10.1002/app.25660
Published online in Wiley InterScience (www.interscience.wiley.com).

ABSTRACT: The pyrolysis of an epoxy resin and the fire behavior of corresponding carbon fiber-reinforced composites, both flame-retarded with either 10-ethyl-9,10-dihydro-9-oxa-10-phosphaphenanthrene 10-oxide or 1,3,5-tris[2-(9,10-dihydro-9-oxa-10-phosphaphenanthrene 10-oxide-10-)ethyl]1,3,5-triazine-2,4,6(1H,3H,5H)-trione, are investigated. The different fire retardancy mechanisms are discussed, and their influence on the fire properties assessed, in particular for flammability (limiting oxygen index, UL 94) and developing fires (cone calorimeter with different external heat fluxes of 35, 50, and 70 kW m^{-2}). Adding the flame retardants containing 9,10-dihydro-9-oxa-10-phosphaphenanthrene-10-oxide affects the fire behavior by both condensed phase and gas phase mechanisms. Interactions between the additives and the epoxy resin result in a change in the decomposition pathways and an increased char formation. The release of phosphorous products results in significant flame inhibition. The fire properties achieved are thus interesting with respect to industrial exploration. © 2007 Wiley Periodicals, Inc. J Appl Polym Sci 104: 2260–2269, 2007

Key words: flame retardance; thermosets; composites; thermogravimetric analysis (TGA); pyrolysis; high performance polymers; epoxy resin

INTRODUCTION

Epoxy resins show advantageous properties with respect to: ease of processing, low cost, good mechanical properties, and environmental advantages. They are commonly used for applications as adhesives in electrical devices as well as for fiber-reinforced composites in the transportation sector. Indeed, their increasing use in the aircraft industry and the increasing fire-protection demands in trains present the challenge of developing halogen-free, flame-retarded epoxy resins for high-performance composites. Several either nonreactive or reactive phosphorus-containing flame retardants have been investigated and have been the subject of recent review articles.[1–3] Phosphorous compounds impart flame retardancy through flame inhibition in the gas phase and char enhancement in the condensed phase.[4–10] One of the compounds that has attracted increasing attention is 9,10-dihydro-9-oxa-10-phospha-phenanthrene-10-oxide (DOPO)[11–16] and its derivatives, enabling significant improvement in the fire behavior of epoxy resins at phosphorus contents as low as 2–3 wt %.

This work contributes to the understanding of the mechanisms and the efficiency of flame retardancy by fundamentally evaluating two different nonreactive 9,10-dihydro-9-oxa-10-phosphaphenanthrene-10-oxide-based flame retardants. In particular, a comprehensive study on pyrolysis is carried out with the objective of figuring out the decomposition pathways of the flame-retarded epoxy resins. The study focuses on decomposition temperatures, char yield, and pyrolysis products as key characteristics in determining the fire retardancy mechanisms and their efficiency in corresponding carbon fiber composites for different fire scenarios and tests. Thus this contribution is one of a series of articles, the previous ones of which covered the processing and curing behavior, mechanical properties, and the fire behavior of pure epoxy resins.[16–18] It is the aim of these studies to work out means of identifying promising compounds that can be incorporated into current curable epoxy formulations to yield fire-resistant, high-performance composite applications. There is a clear need to enhance the flame retardancy of such matrices while maintaining their high mechanical performance, especially

Correspondence to: B. Schartel (bernhard.schartel@bam.de).

Contract grant sponsor: German Science Foundation; contract grant numbers: SCHA 730/6-1, Po 575/8-1, Po 575/8-2, DO 453/4-1, DO 453/4-2, AL 474/4-1, AL 474/4-2.

with regard to delamination resistance, and while maintaining applicability in liquid composite molding techniques such as resin transfer molding (RTM) and resin infusion (RI).

EXPERIMENTAL

Materials

A bifunctional diglycidyl ether of bisphenol-A (DGEBA) monomer (Ruetapox 0162, Bakelite) with an epoxy equivalent weight of 173 g/equiv was used as received. The 4,4′-diaminodiphenylsulphone (DDS) hardener (synthesis grade, Merck) with an amino equivalent weight of 62 g/equiv was also used as received. Two nonreactive flame retardant additives (Fig. 1), 10-ethyl-9,10-dihydro-9-oxa-10-phosphaphenanthrene 10-oxide (DOP-Et) and 1,3,5-tris(2-(9,10-dihydro-9-oxa-10-phosphaphenanthrene 10-oxide-10-) ethyl(1,3,5-triazine-2,4,6(1H,3H,5H)-trione (DOP-Cy), were prepared as reported in Refs. 16 and 19, with a purity exceeding 97% as determined by means of NMR spectroscopy. FTIR of (DOP-Et; cm^{-1}): 1477 (aromatic ring), 1426 (P—C_6H_4), 1204 (P=O), 1117 (P—O—C), 910 (P—O—C), 758 (*o*-disubstituted aromatic ring); FTIR of (DOP-Cy; cm^{-1}): 1676 (C=O), 1460 (*sym*-triazine + aromatic ring), 1427 (P—C_6H_4), 1200 (P=O), 1117 (P—O—C), 906 (P—O—C), 749 (*o*-disubstituted aromatic ring). The corresponding complete FTIR spectra of both compounds are shown later, when the pyrolysis products in the condensed phase are discussed.

Preparation and curing procedure of neat epoxy materials and reinforced composites

The DGEBA resin was placed in a glass flask and heated to 130°C in an oil bath connected to a temperature controller. The desired weight fraction of the additive was added slowly to the resin and mixed with a mechanical stirrer for 30 min at 600 rpm, keeping the temperature constant at 130°C, until the additive was dissolved and the mixture was clear. After the mixture became clear, the required amount of DDS was added (mol ratio DGEBA/DDS = 5 : 2) and dispersed for a further 25 min until the mixture was clear again. The final mixture was poured into a preheated aluminum mold at 130°C and degassed in a programmable vacuum oven at the same temperature for 45–60 min. The mold was coated with a thin layer of Frekote-700 NC for easy release of the cured specimens. The mixtures were then cured according to the following curing cycle: the temperature was increased to 180°C at a heating rate of 2°C/min, held constant for 2 h, and was finally slowly decreased to room temperature. The prepared mixtures contained either 15.7 wt % of DOP-Et or 18.4 wt % of DOP-Cy that correspond to a phosphorus content of 2.0 wt % in either case. A neat DGEBA/DDS resin (ER) was prepared in the same way for the purpose of comparison.

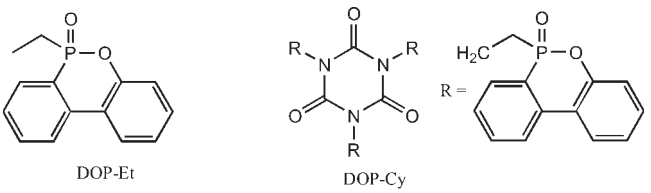

Figure 1 Structures of the flame retardant additives used: DOP-Et and DOP-Cy.

In addition, carbon fiber-reinforced composite plates were manufactured using the vacuum-assisted resin transfer molding (VARTM) technique. The epoxy-based matrices for these composites were prepared according to the procedure outlined above. The reinforcement consisted of eight plies of woven fabric (Atlas 1/4, 5 harness satin, ECC GmbH and CO, fiber aerial weight = 370 g/m^2). A Kapton® film of 13 μm thickness was introduced between the fourth and fifth carbon fabric as a sharp crack starter in the midplane of the composite area designated for further mechanical tests. The fiber reinforcement was placed in the preheated RTM mold at 100°C into which the epoxy mixture was driven by vacuum. The composites were cured at 180°C for 2 h followed by a slow cooling to room temperature. A composite reference based on the nonmodified epoxy system was prepared using an identical experimental procedure. The composite plates contained 60 vol % of fibers, and their quality was verified by ultrasonic C-scans using a HFUS 2400 AirTech from Dr. Hillger with a 16-MHz transducer, as well as by a light microscopy of polished cross sections. The samples are referred to as ER/CF, ER/CF/DOP-Et, and ER/CF/DOP-Cy.

Flammability and fire behavior

The flammability (response to a small flame) of the epoxy composites was studied by both the oxygen index test (limiting oxygen index, LOI) following the ISO 4589 standard and the UL 94 standard, on 2.8-mm-thick specimens in the vertical and horizontal configuration. The fire behavior was investigated with a cone calorimeter according to ISO 5660. Plates, 10×10 mm^2 and of 2.8 mm, thickness were tested in the horizontal sample position with the retainer frame. External heat fluxes (irradiation) of 35, 50, and 70 kW/m^2 were applied. All tests were performed in duplicate.

Thermogravimetry and products of thermal decomposition

Thermogravimetric measurements and the temperature-related release of volatile pyrolysis products of the

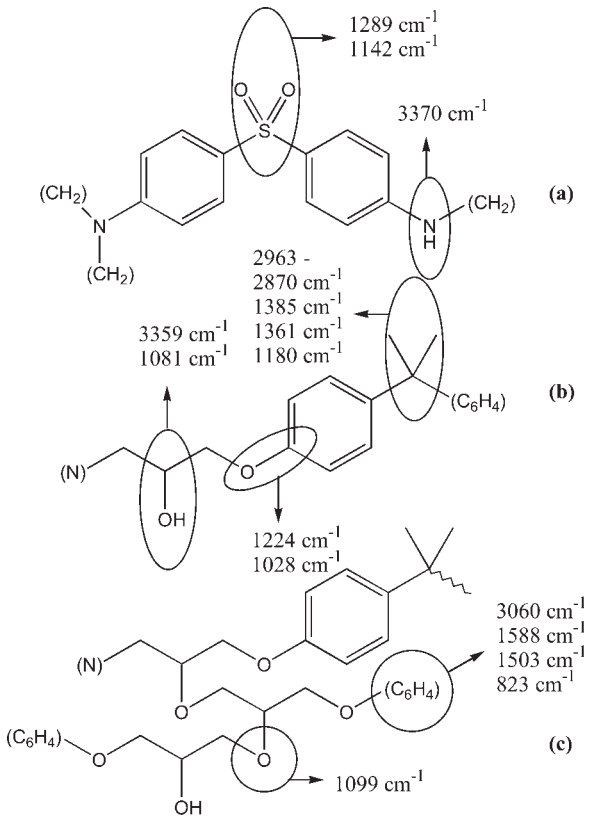

Figure 2 Expected chemical structures obtained during curing of ER mixtures, and origin of the main absorption bands observed in the FTIR spectra.

nonreinforced epoxy resins were studied by means of coupled TG–FTIR spectroscopy (Thermobalance TGA/STDA 851 by Mettler-Toledo, Gieβen, Germany; FTIR-Spectrometer Nexus 470 by Nicolet Instruments, Offenbach, Germany). Standard measurements were performed at a heating rate of 10°C/min under a nitrogen flow of 30 cm^3/min. The nonvolatile residue reproducibility was ± 1 wt %. The sample size was of about 15 mg. A transfer line with an inner diameter of 1 mm heated to 250°C was used to transfer the evolved products into the FTIR cell heated by a heating jacket to 260°C, with an optical path length of 20 cm. The following FTIR conditions were used: resolution of 4 cm^{-1}; scan rate 16; recording frequency of spectra of every 8 s. The TG–FTIR data were evaluated by the OMNIC 5.1b Nicolet program.

In addition, solid residues collected during thermogravimetry were investigated by means of FTIR spectroscopy (FTIR-Spectrometer Nexus 670/870 by Nicolet Instruments) using the Smart Golden Gate Single Reflection Diamond ATR accessory.

RESULTS AND DISCUSSION

Epoxy structure

During the curing process, reactions between the epoxy ring and primary amines produce chain growth giving rise to a secondary hydroxy group and a secondary amine. Chain branching and formation of a network occur in the course of later reactions, involving both the secondary amines and hydroxy groups. Owing to both the deficiency of DDS and the reactivity of the secondary aromatic amine to the epoxy functionality, which is much lower than that of the primary amine,[20] three structures (a), (b), and (c) (Fig. 2) are expected to be formed in the epoxy resin system, with the structure (c) originating from an etherification reaction (epoxide + hydroxy). This is supported by the representative FTIR spectra of the initial epoxy resins, which show a strong absorption band at 1099 cm^{-1} (ER/DOP-Et) or 1101 cm^{-1} (ER/DOP-Cy) because of C—O—C stretching vibration of aliphatic polyether structures.[21]

Mass loss during decomposition

Table I and Figure 3 summarize the most important characteristics of the thermogravimetric results. Figure 3(a) shows the influence of DOP-Et on the thermal decomposition behavior of ER by comparing the experimental curve with the calculated one resulting from the linear combination of the curves of neat ER and neat DOP-Et. The two stages of weight-loss, which both curves exhibit, are associated with the volatilization of DOP-Et and the successive decomposition of ER. Although the onset temperature for weight-loss decreases, the weight-loss process observed at the initial stage of decomposition is retarded, compared to that expected from the calculated curve. There is, however, a decrease in temperature for the main-stage weight-loss process due to a destabilization of ER. In addition, incorporation of DOP-Et slightly increases the amount of the nonvolatile residue ($\Delta m = +2$ wt % in comparison to ER and $\Delta m = +4$ wt % in comparison to the calculated superposition) between 450 and 800°C. The fact that the calculated curve does not coincide with the experimental one is taken as evidence for the interaction of DOP-Et with ER.

The same approach is illustrated for ER/DOP-Cy in Figure 3(b) and Table I. The calculated curve shows two distinct steps due to decomposition of DOP-Cy and ER. However, these steps are hardly separated in

TABLE I
Thermogravimetry Data of DOP-Et, DOP-Cy, ER, ER/DOP-Et, and ER/DOP-Cy

	DOP-Et	DOP-Cy	ER	ER/DOP-Et	ER/DOP-Cy
$T_{10\%}$ (°C)	248	355	397	358	365
T_{max} (°C)	322	362	405	398	396
Δm (%)	98.1	91.9	80.9	78.4	74.9
Residue (800°C)	1.9	3.8	14.7	16.7	19.8

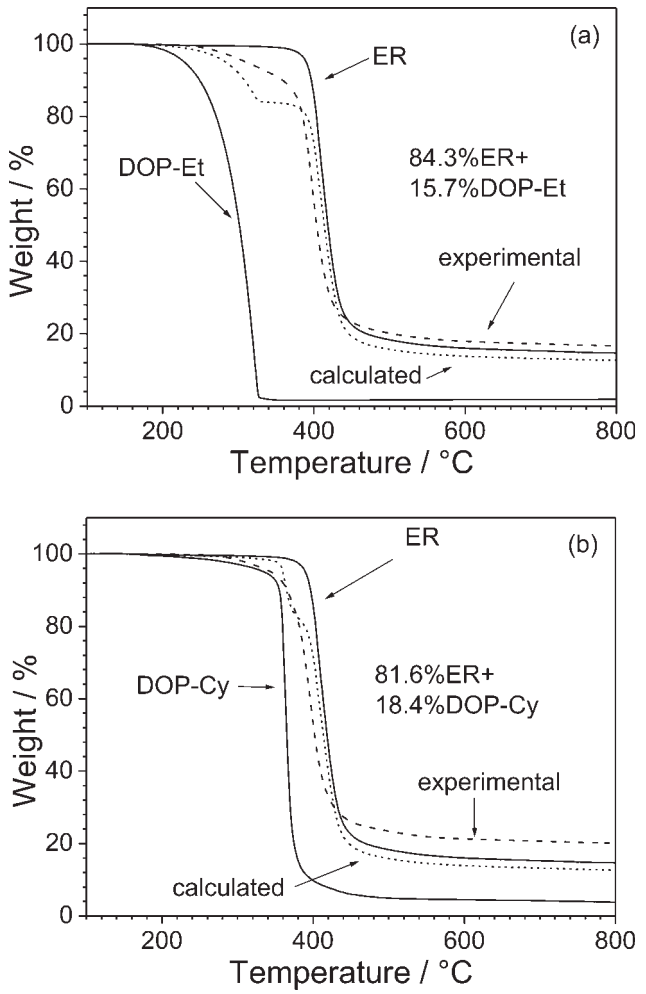

Figure 3 Thermogravimetry under nitrogen at a heating rate of 10°C/min of (a) ER, DOP-Et and their mixture (experimental and calculated) and (b) ER, DOP-Cy, and their mixture (experimental and calculated).

the experimental curve. This thermal behavior can be understood through a destabilizing effect of the decomposition products of DOP-Cy, which reduce the degradation temperature of ER due to interaction. As a further result of this interaction, an increase in the amount of nonvolatile decomposition products ($\Delta m = +5.1$ wt % in comparison to ER and $\Delta m = +7.1$ wt % in comparison to the calculated superposition) is observed between 450 and 800°C.

In first approximation, ER/DOP-Et and ER/DOP-Cy showed similar changes in the thermal decomposition in comparison to the decomposition of ER as well as to the linear combination of the curves of neat compounds. For both systems, an interaction between additive and epoxy occurs, the main decomposition temperature of epoxy is reduced, and the char formation is enhanced. However, there are significant differences in the details. In comparison to the calculated decomposition, the onset temperature of observed decomposition is increased for ER/DOP-Et whereas it is decreased for ER/DOP-Cy, and the increase in char for ER/DOP-Cy is about twice as much as for ER/DOP-Et.

Volatile pyrolysis products

TG–FTIR investigations of ER/DOP-Et showed a strong release of phenol, alkylphenols (*p*-isopropylphenol, bisphenol-A), water, ketone-containing moieties (acetone), and acrolein with representative absorption bands at 746, 827, 3853, 1747, and 1731 cm^{-1}. The differentiation between each type of compound containing phenol implies that nonsubstituted phenol shows a strong 746 cm^{-1} band and a weak-to-medium 827 cm^{-1} band, whereas the alkylphenols exhibit only one band in the same region, at 827 cm^{-1}. The position of other OH- (3650 and 1340 cm^{-1}) and aromatic-related (1605 and 1510 cm^{-1}) bands is quite similar. Acrolein representative absorption bands are 2846–2714, 1731, 1708, 1156, 984, 956, and 922 cm^{-1}, identified by means of the HR Nicolet Vapor Phase Spectra Library.

The release of the pyrolysis products, as a function of temperature, is presented in Figure 4. The thermal decomposition of ER/DOP-Et starts with the evolution of acrolein. The subsequent release of water and acetone indicates primary decomposition of the 2-hydroxytrimethylene segment. Finally, nonsubstituted phenol evolves accompanied by alkyl-containing phenols, indicative of a decomposition of bisphenol A units. The 3017 cm^{-1} band (Fig. 4) represents the two-stage release of methane.

With respect to the epoxy matrix, the sequence in which the volatiles are released from ER/DOP-Cy follows that of ER/DOP-Et (Fig. 5), i.e., acrolein, water and acetone, phenol, alkylphenols and methane, with

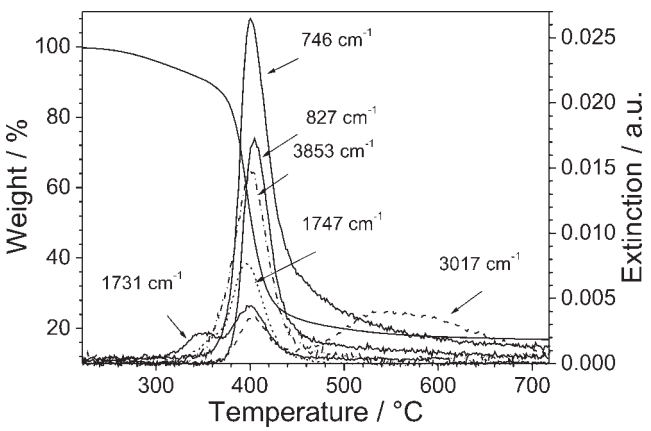

Figure 4 The release of pyrolysis products as a function of temperature during thermogravimetry of ER/DOP-Et, monitored by representative absorption bands: 746 cm^{-1} – phenol, 827 cm^{-1} – alkylphenols, 3853 cm^{-1} – water, 1747 – acetone, 1731 cm^{-1} – acrolein, 3017 cm^{-1} – methane.

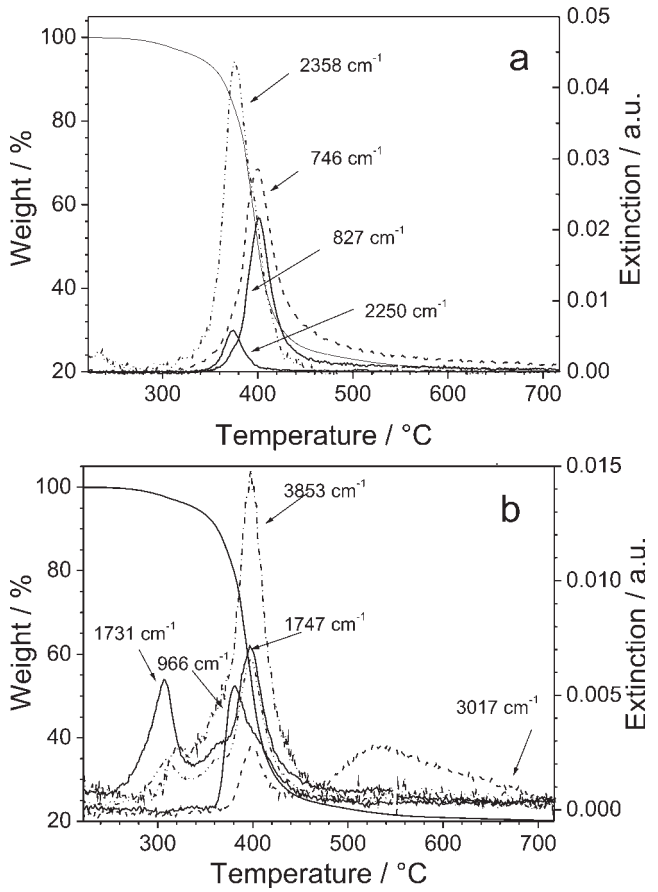

Figure 5 The release of pyrolysis products as a function of temperature during thermogravimetry of ER/DOP-Cy, monitored by representative absorption bands: (a) 746 cm^{-1} – phenol, 827 cm^{-1} – alkylphenols, 2358 cm^{-1} – carbon dioxide, 2250 cm^{-1} – isocyanic acid, (b) 3853 cm^{-1} – water, 966 cm^{-1} – ammonia, 1747 cm^{-1} – acetone, 1731 cm^{-1} – acrolein, 3017 – methane.

the onset of the release of acrolein and water shifted to lower temperatures. The maxima of the peak release rates of water, phenol and alkyl-containing phenols coincide in the two epoxy resins.

In addition, pyrolysis of ER/DOP-Cy produced further products traced by 966, 2358, and 2250 cm^{-1}, characteristic of ammonia, carbon dioxide, and isocyanic acid. The maxima of their evolution are observed between those of acrolein and phenols. The products are indicative of the decomposition of the *sym*-triazine ring of DOP-Cy.

Nonvolatile decomposition products

FTIR spectra of the pyrolysis residues of ER/DOP-Et are shown in Figure 6, spectra c–h. The attribution of the main epoxy-related absorption bands in the initial spectrum (Fig. 6, spectrum b) was outlined in Figure 2. The 911 cm^{-1} band (Fig. 6, spectrum a) is chosen to mark DOP-Et; the cured ER does not exhibit any absorption bands in this spectral region.

The heating of ER/DOP-Et results in a steady vanishing of the 911 cm^{-1} band, indicating volatilization of DOP-Et. It should be noted that the elimination of the band is retarded, as it is still present at 30 wt % (Fig. 6, spectrum d) of the initial mixture containing about 16 wt % DOP-Et. The initial removal of the additive is supplemented by the appearance of olefinic compounds (the corresponding C=C stretching vibration at 1650 cm^{-1}; Fig. 6, spectrum c) that disappear on further heating.

Starting from 10% weight-loss, significant modifications in the epoxy network are observed (Fig. 6, spectra c–f). There is a decrease in the intensity of the —OH-related bonds (3359 and 1080 cm^{-1}) and alkyl–aryl ether bonds (1227 and 1025 cm^{-1}), indicating preferential decomposition of the 2-hydroxytrimethylene structure [i.e., structure similar to Fig. 2(b)] and its volatilization along with the bisphenol A unit. Simultaneously, a relative increase in the intensity of secondary amines (3370 cm^{-1} and corresponding DDS-related bands at 1289 and 1142 cm^{-1}, which can be regarded as an internal standard at these stages of decomposition) and a dialkyl ether band (1099 cm^{-1}; there also is a small contribution of DDS due to the C—S stretching vibration) are observed, indicative of an accumulation of the 2-alkoxy-3-phenoxy-1-phenylaminylpropane structure [i.e., structure similar to Fig. 2(a) and in part to Fig. 2(c)]. The process reaches its maximum at 65% weight loss (Fig. 6, spectrum f).

After 65% weight loss, dramatic changes are noticed in all spectral regions. The secondary amines and aliphatic polyether absorption bands disappear. A new absorption band at 1254 cm^{-1} developed, associated with the formation of diaryl ethers. A complex

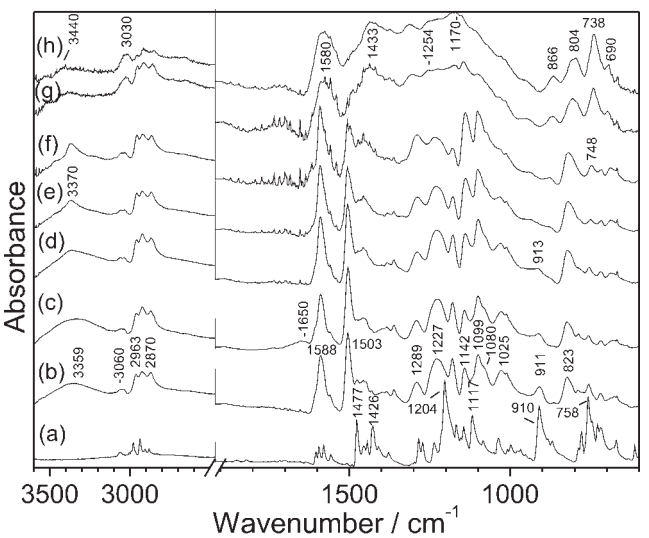

Figure 6 FTIR spectra of DOP-Et (a), ER/DOP-Et (b), and solid products of thermal decomposition of ER/DOP-Et, collected in thermogravimetry at 10% (c), 30% (d), 50% (e), 65% (f), 80% (g) weight-loss and at 565°C (h).

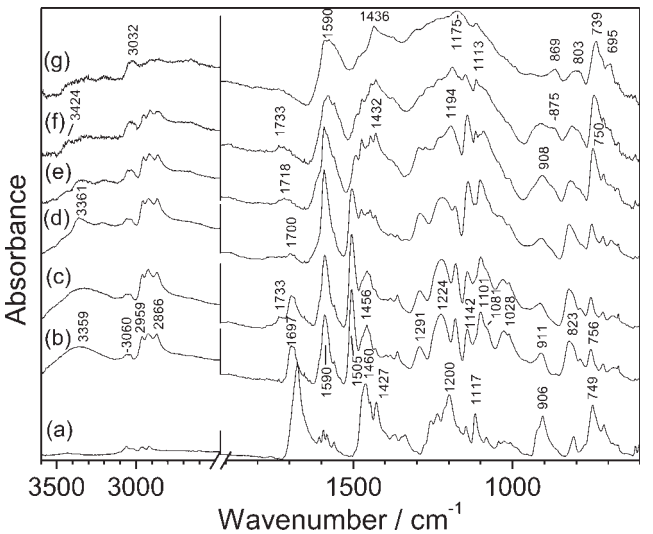

Figure 7 FTIR spectra of DOP-Cy (a), ER/DOP-Cy (b), and solid products of thermal decomposition of ER/DOP-Cy collected in thermogravimetry at 7% (c), 40% (d), 70% weight-loss (e), at 495°C (f), and 565°C (g) (see the TGA curve in Fig. 3(a) for the identification of the samples).

absorption at 866–690 cm^{-1} becomes increasingly important due to the wagging vibrations of isolated aromatic CH groups, indicating that polysubstitution of the aromatic rings is proceeding. The aromatic ring C=C stretching vibration at 1503 cm^{-1} disappears and that at 1580 cm^{-1} becomes broader, indicating the formation of polyaromatic carbons. The weak absorption band of residual phenols at 3440 cm^{-1} is still observed at the end of the temperature treatment (Fig. 6, spectrum h).

The chemical transformations of the epoxy network of the ER/DOP-Cy mixture (Fig. 7, spectra b–g) follow those of the ER/DOP-Et mixture. The main differences appear in the interpretation of the thermal behavior of the additives. While volatilization of DOP-Et is observed during pyrolysis of ER/DOP-Et, completed at 50% weight-loss, DOP-Cy undergoes decomposition. This is evident from the development of the 1733 cm^{-1} band (Fig. 7, spectrum c) ascribable to the C=O stretching vibration of the cyanuric acid (1,3,5-triazine-2,4,6(1H,3H,5H)-trione) moieties. A small amount of the *sym*-triazine ring of DOP-Cy persisted heating to 40% weight loss (Fig. 7, spectrum d); however, the 1700 cm^{-1} band may have some contribution from carbonyl-containing structures resulting from decomposition of the 2-hydroxypropylidene structure. Furthermore, the DOPO structure released during the decomposition of DOP-Cy is partially retained in the residue. The corresponding absorption bands at 1432, 1194, 1113, and 908 cm^{-1} can be found even at 495°C (Fig. 7, spectrum f), indicating that the structure can be either implemented in the decomposition products of ER or polymerized.

Proposed pyrolysis pathways and interactions between ER and the flame retardants

The cured ER/DOP-Et and ER/DOP-Cy mixtures exhibit a quite unusual thermal decomposition behavior that can not be expected for nonreactive additives. The first piece of evidence comes from TG analysis, which reveals occurrence of an interaction of the additives with ER during pyrolysis. This conclusion is further supported by the FTIR study of volatile decomposition products, which reveals formation of acrolein, preceding that of water and acetone. The onset and the peak release temperature for the evolution of water and acetone decreases compared to those of a pure ER. Finally, volatilization of the ethyl dihydrooxaphosphaphenanthrene structure is strongly retarded for ER/DOP-Et, as shown by the FTIR study of the nonvolatile decomposition products. Comparable results illustrating an influence of compounds containing DOPO on the decomposition pathway of ER have been reported before.[22]

The pyrolysis of methylenedianiline-cured DGEBA yields acrolein at 450°C (0.22% yield); however, it does not occur at 350°C.[23] The pyrolysis of ER/DOP-Et and ER/DOP-Cy produces acrolein starting at 300°C (DOP-Et) or 250°C (DOP-Cy). One of the possible ways to form acrolein is the decomposition of the polyether structure c (Fig. 2).[23] The structure accumulates by heating (Fig. 6, spectrum f) and may account for the high temperature evolution of acrolein, as described in Ref. 23. It is also known[24] that the epoxide may isomerize into an aldehyde group that may split off acrolein at a lower temperature (Fig. 8, path d). Formation of the aldehyde-containing structures is favored by the excess of DGEBA and by dilution of the reactive groups by either DOP-Et or DOP-Cy. The presence of an acid formation, which is discussed later, is likely to facilitate the decomposition of the aldehyde and to cause the earlier evolution of acrolein in ER/DOP-Cy.

The effect of DOP-Et may consist in catalyzing the elimination of water from the epoxy network by dehydrating secondary hydroxy groups to produce olefinic bonds in the solid residue (Fig. 6, spectrum c). The olefins created are regarded in the pyrolysis chemistry of epoxy resins as weak sides to initiate the decomposition of the epoxy matrix.

Considering the pyrolysis of ER/DOP-Cy, a peculiarity is observed, as volatile products evolve at lower temperatures than they do through heating ER/DOP-Et, and this implies another initiating mechanism. In trying to find a possible explanation, attention should be paid to the thermal instability of DOP-Cy just above 200°C [Fig. 3(b)]. It is proposed to originate from the fragile N–C linkage, as the FTIR spectrum of solid decomposition products of pure DOP-Cy shows the C=O stretching vibration of isocyanuric acid at

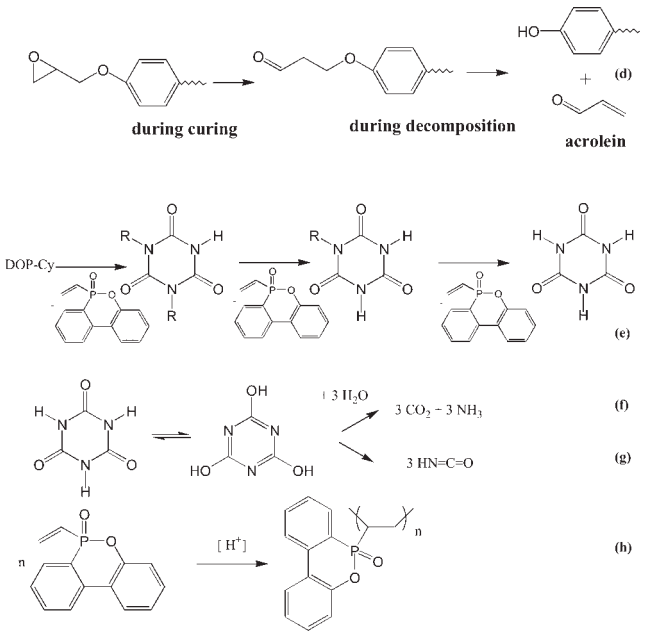

Figure 8 Proposed schemes of the formation of acrolein during pyrolysis of ER/DOP-Et or ER/DOP-Cy (path d), and of the pyrolysis of DOP-Cy (paths e–h).

1723 cm^{-1} (not shown) due to dealkylation of the ethenyl dihydrooxaphospha phenanthrene structure (Fig. 8, path e). The formation of isocyanuric acid causes a decrease in the pH-value, and thus acid-catalyzed dehydration of the 2-hydroxypropylidene structure. In its turn, the evolved water hydrolyzes the cyanuric acid to produce ammonia and carbon dioxide (Fig. 8, path f). The nonhydrolyzed decomposition of cyanuric acid yields isocyanic acid (Fig. 8, path g).[25]

The released 10-ethenyl-9,10-dihydro-9-oxa-10-phosphaphenanthrene 10-oxide (Fig. 8, path e) is as volatile as DOP-Et. However, because of the double bond, it can undergo acid-catalyzed oligomerization reactions (Fig. 8, path h), thus retaining residue in pyrolysis (Fig. 7, spectra e and f). The other possibility of trapping 10-ethenyl-9,10-dihydro-9-oxa-10-phosphaphenanthrene 10-oxide in the solid decomposition products is an acid-catalyzed addition on the aromatic ring of phenolic moieties formed during decomposition of the epoxy structure.

Both ER/DOP-Et and ER/DOP-Cy show the main weight-loss as a result of the volatilization of aromatic and aliphatic parts of the epoxy molecular unit, the main fragments of which are listed in Table II. Structure 1 can be volatilized as aniline (2 mol) and SO_2, whereas structure 2 is volatilized as bisphenol A or its degradation products, i.e., phenol and *p*-isopropenylphenol. Structures 3 and 4 can produce either acetone or water and propylene. Nonvolatilized structures contribute to solid decomposition products. The fact that the pyrolysis of pure DGEBA/DDS yields 19.1 wt % solid residue (Table I) can be explained through the trapping of three 2b structures due to solid phase reactions, the initial relative weight fraction of which is 6.1 wt % (Table II). Instead of one 2b structure, 2a can be utilized due to the alkylation reaction by 3a.[26]

Promotion of the solid decomposition products yield by DOP-Et to 25.6 wt % (21.6 wt % after the main stage of weight-loss recalculated by 1/0.843 for pure ER) indicates that an additional fragment 2b is involved in the charring process. ER/DOP-Cy yields 25.1 wt % char after the main stage of weight loss, 1 wt % of which is due to the decomposition products of DOP-Cy. The corrected char yield is 29.5 wt % (24.1 wt % recalculated by 1/0.816 for pure ER) which is indicative of the involvement of an additional structure 2b and two additional structures 3a.

These results show that the possible charring processes can come from polymerization (or trimerization) of the olefinic bond of *p*-isopropenylphenol units. The structure 2a also can participate through addition to the olefinic structure 3a, leading to polysubstitution. In the case of DOP-Cy, two structures 3a may be involved in charring due to the alkylation of the phenolic ring. Another reaction to trap aromatics in the solid residue may occur through an OH···OH condensation mechanism, yielding diphenyl ether linkages. The FTIR study supports these mechanisms by detec-

TABLE II
Fragments Integrated in the Molecular Unit of DGEBA/DDS

Item	Formula	M_w (g/mol)	Number of units	Weight of units (g)	Wt % of units	Wt % per unit
1	$-HN-C_6H_4-SO_2-C_6H_4-N-$	245	2	490	22.3	11.2
2[a]	$-O-C_6H_4-C(CH_3)_2-C_6H_4-O-$	226	5	1130	51.5	10.3
2a	$-O-C_6H_5$	93	5			4.2
2b	$-O-C_6H_4-C(=CH_2)CH_3$	133	5			6.1
3	$-CH_2-CH(OH)-CH_2-$	58	6	348	15.8	2.6
3a	$-CH=CH-CH_2-$	40	6			1.8
3b	H_2O	18	6			0.8
4	$-CH_2-CH(O-)-CH_2-$	57	4	228	10.4	2.5
				Σ2196	*Σ100*	

[a] Structure 2 can be substituted by structures 2a + 2b; structure 3 can be substituted by structures 3a + 3b.

TABLE III
Flammability Data and Fire Characteristics of the Carbon Fiber-Reinforced Composites ER/CF, ER/CF/DOP-Et, and ER/CF/DOP-Cy

	Error	ER/CF	ER/CF/DOP-Et	ER/CF/DOP-Cy
Flammability				
LOI (%)	±2[a]	31	44	49
UL 94		HB, V1[b]	V1	V0
Cone calorimeter				
t_{ig} (s; at 35 kW/m^2)	±2	122	108	111
THE (MJ/m^2)	±1.0	25.0	15.4	17.0
Peak of HRR (kW/m^2; at 50 kW/m^2)	±7	376	226	252
THE/TML (MJ/m^2 g)	±0.05	2.21	1.55	1.71
Residue (wt %)	±1.0	73.1	76.6	77.0
CO yield (g/g)	±0.005	0.049	0.146	0.136

The cone calorimeter data were averaged for six or two measurements performed, respectively, depending on whether the result is reasonable for all irradiations or characteristic for a certain irradiation.

[a] The error for the LOI determined with test specimens from the same batch of composite materials is <1.

[b] The UL 94 classification was determined twice using two different batches of composite materials.

tion of both polyaromatization of the residue and the formation of diaryl ethers.

With respect to the pyrolysis during fire, which corresponds to the main decomposition step, the major results are:

the onset and maximum decomposition temperature of ER/DOP-Et and ER/DOP-Cy, respectively, are decreased
the char yield is ordered: ER/DOP-Cy > ER/DOP-Et > ER. The absolute increase is rather small (≤5 wt %) and corresponds to a relative decrease in fuel yield of about 3% (ER/DOP-Et) and 7% (ER/DOP-Cy)
ER/DOP-Et releases phosphorus products containing phosphorus efficiently in the gas phase, whereas a partial release of products containing phosphorus is observed for ER/DOP-Cy.

Fire behavior

ER/CF, ER/CF/DOP-Et, and ER/CF/DOP-Cy showed self-extinguishing behavior in the UL94 classification and corresponding high LOI values above 30% (Table III). In comparison to the results for ER/CF composites, the addition of the nonreactive DOPO-compounds increased the LOI by about 13% to 18%. This convincing improvement in flammability behavior is due to a phosphorus concentration of only 2 wt % with respect to the epoxy matrix. For the ER/CF/DOP-Cy, the UL 94 rating improved from a V1 to a V0 classification. Despite the prevention of a sustained flame as a response to small flame (flammability) by adding DOPO compounds, the time to ignition (t_{ig}) decreased (Table III), which is a measure for increasing ignitability. It is ordered: ER/CF > ER/CF/DOP-Cy > ER/CF/DOP-Et. This result corresponds with the decreasing onset and maximum of decomposition monitored by thermal analysis. An increase in thermal stability as such is ruled out as an active flame retardancy mechanism.

Both DOPO compounds crucially reduced the heat release in a developing fire, as reflected by cone calorimeter experiments. Table III summarizes some representative key results of the cone calorimeter investigations. Figure 9 shows the heat release rate (HRR) and the total heat release rate (THR) for a cone calorimeter test performed with an irradiation of 35 and 50 kW/m^2. Figure 10 shows the t_{ig} and the peak of HRR as a function of the applied irradiation. Fire growth characteristics such as the peak of HRR, as well as fire load characteristics such as the total heat evolved (THE) were reduced by more than a third. The significant increase in residue and the decrease in

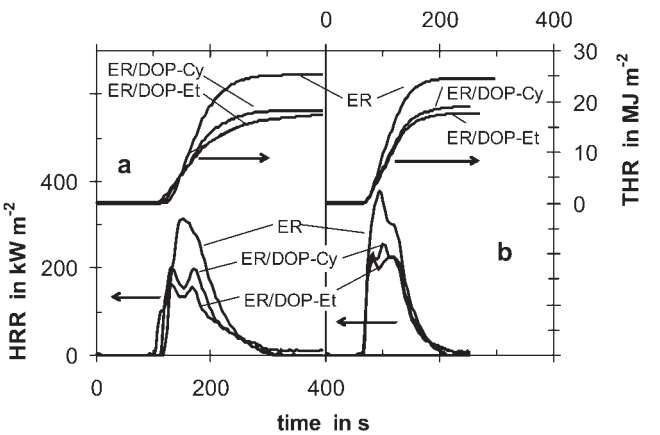

Figure 9 HRR and THR for ER/CF, ER/CF/DOP-Et, and ER/CF/DOP-Cy at irradiation of (a) 35 kW/m^2 and (b) 50 kW/m^2.

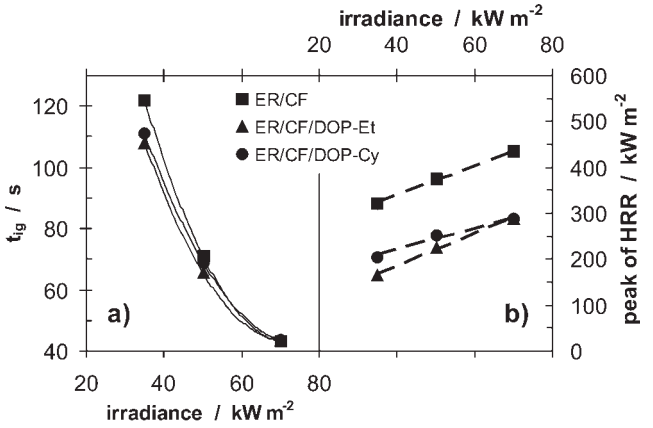

Figure 10 t_{ig} (a) and peak of HRR (b) for ER/CF, ER/CF/DOP-Et, and ER/CF/DOP-Cy at different irradiations.

the quotient of THE/total mass loss indicate simultaneously active condensed phase and gas phase flame retardant mechanisms. The additional charring in the condensed phase results in a decrease of fuel yield per polymer content of about 13–14 wt %, taking into account the fiber content of 60 vol %. When DOPO compounds are added, the char yield and the increase in char yields are systematically higher than the char yield observed in the TG experiments, but show two similar effects. First, adding DOPO compounds results in an increase in char yield; second, the increase is larger for DOP-Cy than for DOP-Et. The reduction of THE/TML indicates flame inhibition in the gas phase of about 30% (ER/CF/DOP-Et) and 23% (ER/CF/DOP-Cy). The flame inhibition as such and the effect being larger for DOP-Et than for DOP-Cy is due to vaporized phosphorus volatiles containing phosphorus and their release rates, both observed in the thermal analysis. The resulting incomplete combustion was also reflected by the increase in CO yield. The reduction of both the fuel amount and its combustion efficiency offers a good explanation for the resulting overall reduction in fire risk such as the heat release during developing fires as monitored in the cone calorimeter, but also the improved flammability properties reflected by LOI and UL 94.

As already discussed, there is a clear improvement for ER/CF/DOP-Et and ER/CF/DOP-Cy in comparison with ER/CF, but the fire behavior of ER/CF/DOP-Et and ER/CF/DOP-Cy is rather similar. With respect to flammability properties, it seems that DOP-Cy is better than DOP-Et. However, a rather large deviation for the flammability behavior was found for different batches of composites, which is of the same order of magnitude. Thus this result must not be over-interpreted. In the cone calorimeter test, it appears that the ER/CF/DOP-Cy shows slightly superior char formation, whereas ER/CF/DOP-Et shows more efficient gas phase activity. Both results agree with the TG results. Since in these systems the gas phase activity was roughly twice as important as char formation with respect to the corresponding heat release reduction, ER/CF/DOP-Et showed the superior performance. However, some of the differences between the two fire-retarded systems are of the same order of magnitude as the error of the data, which is caused by the fact that 60% of the volume is carbon fiber and the differences due to the two additives in the remaining material simply may not be significant enough.

Mechanical behavior

This study targets flame-retarded high-performance composites for which the combination of flame retardancy, adequate processing, and mechanical properties is indeed a challenge. Neither of the two nonreactive organo-phosphorous compounds significantly affected the viscosity and hence the processability of the composite matrix at the studied phosphorus concentration.

The mechanical properties of the composites were evaluated in detail and some of the most important key data are summarized in Table IV. The fracture mechanical studies have been presented in detail in previous publications[23,24] from which the data were taken. As shown in Table IV, neither of the organo-phosphorus compounds significantly affected the overall mechanical performance of the modified composites. Critical mechanical properties such as

TABLE IV
Mechanical Properties of the Composites. Data taken from Refs. 17 and 18

	ER/CF	ER/CF/DOP-Et	ER/CF/DOP-Cy
Flexural properties			
Modulus (GPa)	63 ± 4	65 ± 6	62 ± 1
Strength (MPa)	940 ± 80	1030 ± 100	1040 ± 40
Apparent interlaminar shear strength			
ILSS (MPa)	69 ± 5	69 ± 3	69 ± 6
Interlaminar fracture toughness in mode I and mode II			
G_{Ic} (J/m^2) initiation	603 ± 64	716 ± 118	609 ± 72
G_{Ic} (J/m^2) propagation	740 ± 37	826 ± 35	706 ± 35
G_{Ic} (J/m^2) initiation	588 ± 92	766 ± 24	667 ± 128
G_{Ic} (J/m^2) propagation	1238 ± 196	1381 ± 290	1351 ± 205

delamination resistance in mode I (tension) or mode II (shear) were maintained on a level comparable to that of the unmodified system. The flexural properties and the interlaminar bonding strength (ILSS) were not affected within the experimental error of measurement. Hence, the compounds containing phosphorus under evaluation here were incorporated into the epoxy matrix, providing effective flame retardancy to the composite while maintaining its ease of processing, and physical and mechanical properties at a suitable level for demanding applications.

CONCLUSIONS

The pyrolysis and the fire behavior are investigated for ER (epoxy resin) and corresponding ER/CF (high-performance carbon fiber-reinforced composites), both flame-retarded with the additives DOP-Et and DOP-Cy. Both flame retardants show an interaction in the condensed phase influencing the decomposition of ER. The decomposition pathways of the different materials were investigated in detail with a discussion of the mass loss, the decomposition temperatures, the evolved gases, and the chemical composition of the residues for different conversion and temperature. The onset and maximum decomposition temperatures are decreased, the char yield is increased, and phosphorous volatiles are released. The decreased decomposition temperature results in a decreased ignition resistance of ER/CF. The increased char yield and the release of compounds containing phosphorus crucially improve the flammability and fire properties of ER/CF demonstrated with LOI, UL 94, and cone calorimeter, respectively. For both flame retardants two main mechanisms, char enhancement and flame inhibition, affect fire behavior. DOP-Et shows the more efficient release of phosphorus compounds, but DOP-Cy the higher charring. The flame inhibition was identified to be more important, especially in terms of flammability. The fire properties achieved are interesting with respect to industrial exploration, particularly since the mechanical characteristics did not deteriorate.

The use of DOPO-based flame retardants results in the release of PO into the gas phase and in phosphorus remaining in the condensed phase during pyrolysis. The release of PO results in an efficient flame inhibition, whereas phosphorus in the condensed phase enhances char formation. To what extent which effect occurs depends not only on the chemical structure of the DOPO-compounds but also on the interactions with the polymer and further additives during thermal decomposition. Significant differences are achieved in terms of flame retardancy mechanism and efficiency by using different DOPO-based flame retardants with the same phosphorus content. Tailored DOPO-based flame retardants enable efficient flame retardancy at very low P-contents in the order of 2 wt %. In general, DOPO-based flame retardants show a high propensity to achieve efficient flame inhibition, since the DOPO structure act as precursor for the release of PO during pyrolysis. Hence, DOPO-based flame retardants are especially suitable to be used for materials and protection goals, where a gas phase mechanism is favored, such as highly filled materials or passing flammability test.

References

1. Lu, S. Y.; Hamerton, I. Prog Polym Sci 2002, 27, 1661.
2. Levchik, S. V.; Weil, E. D. Polym Int 2004, 53, 1901.
3. Levchik, S.; Piotrowski, A.; Weil, E.; Yao, Q. Polym Degrad Stab 2005, 88, 57.
4. Lewin, M.; Weil, E. D. In Fire Retardant Materials; Horrocks, A. R.; Price, D., Eds.; Woodhead Publishing: Cambridge, UK, 2001; p 31.
5. Hastie, J. W. J Res Natl Bur Stand Sect A Phys Chem 1973, 77, 733.
6. Green, J. In Fire Retardancy of Polymeric Materials; Grand, A. F.; Wilkie, C. A., Eds.; Marcel Dekker: New York, 2000; Chapter 5.
7. Schartel, B.; Braun, U. e-Polymers 2003, art. no. 013.
8. Schartel, B.; Kunze, R.; Neubert, D. J Appl Polym Sci 2002, 83, 2060.
9. Braun, U.; Schartel, B. Macromol Chem Phys 2004, 205, 2185.
10. Davis, J.; Huggard, M. J Vinyl Additive Technol 1996, 2, 69.
11. Shieh, J. Y.; Wang, C. S. J Polym Sci Part A: Polym Chem 2002, 40, 369.
12. Lin, C. H.; Wang, C. S. Polymer 2001, 42, 1869.
13. Hussain, M.; Varley, R. J.; Mathus, M.; Burchill, P.; Simon, G. P. J Mater Sci Lett 2003, 22, 455.
14. Shieh, J. Y.; Wang, C. S. Polymer 2001, 42, 7617.
15. Wang, C. S.; Lin, C. H. J Polym Sci Part A: Polym Chem 1999, 37, 3903.
16. Perez, R. M.; Sandler, J. K. W.; Altstädt, V.; Hoffmann, T.; Pospiech, D.; Ciesielski, M.; Döring, M. J Mater Sci 2006, 41, 341.
17. Perez, R. M.; Sandler, J. K. W.; Altstädt, V.; Hoffmann, T.; Pospiech, D.; Ciesielski, M.; Döring, M.; Braun, U.; Knoll, U.; B. Schartel, B. J Mater Sci 2006, 41, 4981.
18. Perez, R. M.; Sandler, J. K. W.; Altstädt, V.; Hoffmann, T.; Pospiech, D.; Ciesielski, M.; Döring, M.; Braun, U. B.; Schartel, B. In Advances in the Flame Retardancy of Polymeric Materials: Current Perspectives, Presented at the FRPM'05; Schartel, B., Ed.; Chapter 5, to appear.
19. Dittrich, U.; Just, B.; Döring, M.; Ciesielski, M. Eur. Pat. 1,512,690 (2004).
20. Riccardi, C. C.; Williams, R. J. J. In Crosslinked Epoxies; Sedláček, B.; Kahovek, J., Eds.; Walter DeGruyter: Berlin, 1987; p 291.
21. Colthup, N. B.; Daly, L. H.; Wiberley, S. E. Introduction to Infrared and Raman Spectroscopy, 3rd ed.; Academic Press: London, 1990.
22. Braun, U.; Knoll, U.; Schartel, B.; Hoffmann, T.; Pospiech, D.; Artner, J.; Ciesielski, M.; Döring, M.; Perez-Graterol, R.; Sandler, J. K. W.; Altstädt, V. Macromol Chem Phys 2006, 207, 1501.
23. Lee, L. H. J Polym Sci Part A: Gen Pap 1965, 3, 859.
24. Anderson, H. C. Polymer 1961, 2, 451.
25. Shimasaki, C.; Morikoshi, T.; Nakayama, H.; Takakura, M.; Ono, S.; Yoshimura, T.; Morita, H.; Tsukurimichi, E. Nippon Kagaku Kaishi 1996, 4, 389.
26. March, J. Advanced Organic Chemistry: Reactions, Mechanisms, and Structure, 4th ed.; Wiley: New York, 1992.